Scheme III

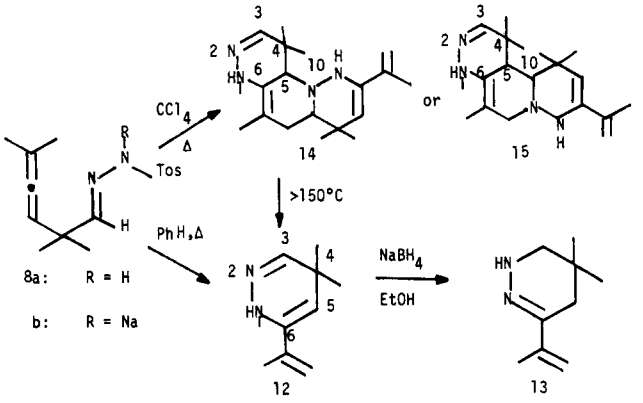

gives a 38% yield of a dimer of **12**, with spectroscopic properties[5] in accord with the structure **14** or, less satisfactorily, structure **15**.[6] The dimer decomposes to the monomer **12** upon gas chromatography (GC) on an OV-101 column (injector at 250 °C, column temperature 150 °C).[7]

In the reactions of Scheme II 3,3-dimethylcyclopropene (**16**), 1,3,3-trimethylcyclopropene (**17**), and 1,2,3,3-tetramethylcyclopropene (**18**) give rise to the products shown in Table I. The two most likely pathways for allene formation are illustrated for the product from **16**: (i) addition of the α-bromoalkenyllithium **19** or the THF-derived diazo-oxonium zwitterion-**20**[2] to the cyclopropene followed by fragmentation or (ii) addition of a carbenoid **9** to give an isopropylidenebicyclo[1.1.0]butane (**21**) followed by a thermal decomposition analogous to the bicyclo[1.1.0]butane → 1,3-butadiene reaction.[8] Further work will be required to establish the mechanism of this reaction.

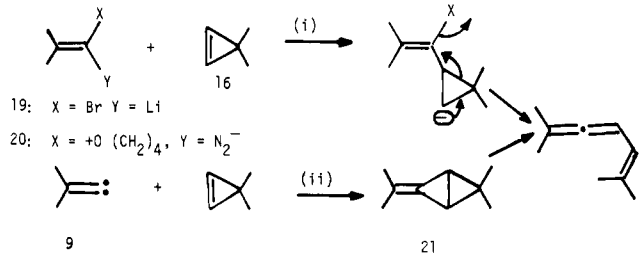

The key observation of Table I is the formation of the dihydropyridazine **12**, the same substance obtained earlier from the *p*-toluenesulfonylhydrazonate **8b** (Scheme III). A plausible rationale (Scheme IV) would involve capture of the diazoethene intermediate **6**, previously postulated[2] to be formed in the acetone–diazomethyl phosphonate reaction, to give the 1,3-addition product **22**. The latter species can intersect the pathway which originates in the hydrazonate **8b** by any of several reactions (Scheme IV).

The present results suggest that the normally reversible 1,1-addition of diazoalkanes[9,10] can be driven to completion if a suitable trapping process (e.g., hydrogen shift) is available (see Scheme IV, **22–24** → **12**). They also provide the first example of the dipolarophilic interception of a nitrogenous intermediate in the

Scheme IV

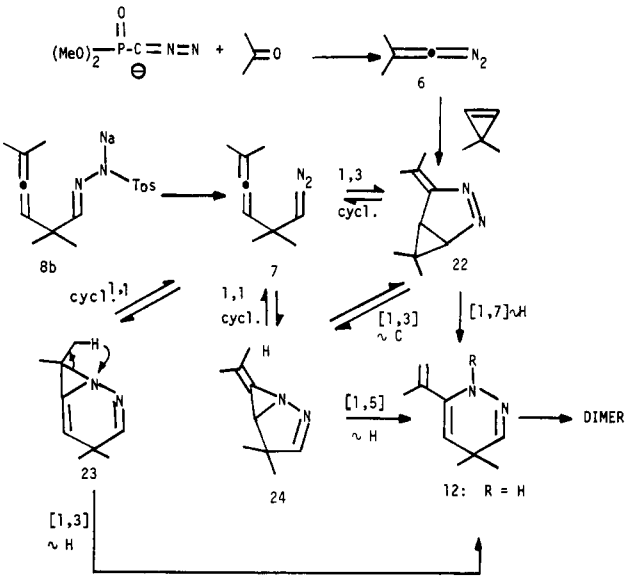

diazomethyl phosphonate–ketone–olefin reaction. The observation that this same adduct is obtained from the phosphorus-free precursor **8b** constitutes strong presumptive evidence in support of the proposed[2,3] free diazoethene intermediate.

Acknowledgment. We are grateful to the National Science Foundation (CHE-8011399) and the National Institute of General Medical Sciences (GM-23375) for partial support of this research. We also thank the National Science Foundation (CHE-7916210) for its support of the NSF Regional NMR Facility at Yale University and Professor Richard D. Adams for the X-ray structure determination.

Supplementary Material Available: Spectroscopic data characterizing compounds **12** and **14**. Details of X-ray crystallographic analysis of compound **12**, diagrams of bond angles and distances, and a listing of atomic positional and thermal parameters (5 pages). Ordering information is given on any current masthead page.

(6) Although the choice is not crucial here, we favor structure **14** for the dimer on the basis of both the ^1H and the ^{13}C NMR spectra.[5]

(7) Heating monomer **12** in pure CCl_4 does not produce dimer **14**, whose formation from the salt **8b** in that solvent therefore presumably involves a catalytic mechanism in which **12** is formed but does not survive the (basic) conditions of the hydrazonate decomposition.

(8) (a) Srinivasan, R. *J. Am. Chem. Soc.* **1963**, *85*, 4045. (b) Closs, G. L.; Pfeffer, P. E. *Ibid.* **1968**, *90*, 2452. (c) Wiberg, K. B.; Lavanish, J. M. *Ibid.* **1966**, *88*, 5272. (d) Wiberg, K. B.; Szeimies, G. *Tetrahedron Lett.* **1968**, 1235. (e) Frey, H. M.; Stevens, I. D. R. *Trans. Faraday Soc.* **1965**, *61*, 90. (f) Srinivasan, R.; Levi, A. A.; Haller, I. *J. Phys. Chem.* **1965**, *69*, 1775.

(9) (a) Padwa, A.; Ku, H. *Tetrahedron Lett.* **1980**, 1009. (b) Padwa, A.; Rodriguez, A. *Ibid.* **1981**, 187.

(10) Miyashi, T.; Nishizawa, Y.; Sugiyama, T.; Mukai, T. *J. Am. Chem. Soc.* **1977**, *99*, 6109; (b) Nishizawa, Y.; Miyashi, T.; Mukai, T. *Ibid.* **1980**, *102*, 1176; (c) Miyashi, T.; Fujii, Y.; Nishizawa, Y.; Mukai, T. *Ibid.* **1981**, *103*, 725.

Kinetic Bistability in the Permanganate Oxidation of Oxalate

John S. Reckley and Kenneth Showalter*

Department of Chemistry, West Virginia University
Morgantown, West Virginia 26506

Received July 20, 1981

A chemical reaction carried out in a continuous flow stirred tank reactor (CSTR) may exhibit more than one stationary state at a particular pumping rate, provided the kinetics of the reaction are appropriately nonlinear. Steady-state multiplicity is a phenomenon of considerable intrinsic interest and is important to our understanding of chemical dynamics in systems far removed from equilibrium. Of the few isothermal chemical systems known to exhibit kinetic bistability, only the acidic bromate oxidation of cerium(III) is understood in detail.[1] Bistability has been recently discovered in the iodate oxidation of arsenous acid and significant progress has been made toward explaining the behavior in terms of elementary chemical reactions.[2,3] In this communication, we

(1) (a) Geiseler, H.; Föllner, H. H. *Biophys. Chem.* **1977**, *6*, 107–115. (b) Bar-Eli, K.; Noyes, R. M. *J. Phys. Chem.* **1978**, *82*, 1352–1359.

(2) Papsin, G. A.; Hanna, A.; Showalter, K. *J. Phys. Chem.* **1981**, *85*, 2575–2582.

0002-7863/81/1503-7012$01.25/0

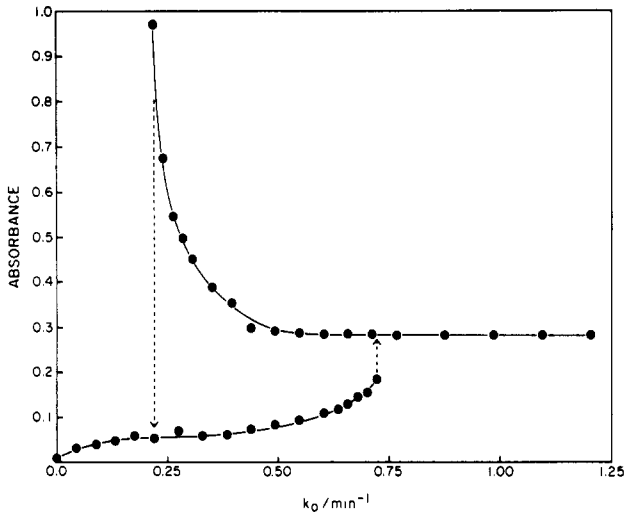

Figure 1. Optical absorbance at 400 nm as a function of k_0. Path length 1.0 cm. Reactant concentrations: $[KMnO_4]_0 = 2.55 \times 10^{-3}$ M, $[Na_2C_2O_4]_0 = 7.64 \times 10^{-3}$ M, and $[H_2SO_4]_0 = 5.09 \times 10^{-2}$ M. Temperature: 25.0 ± 0.1 °C.

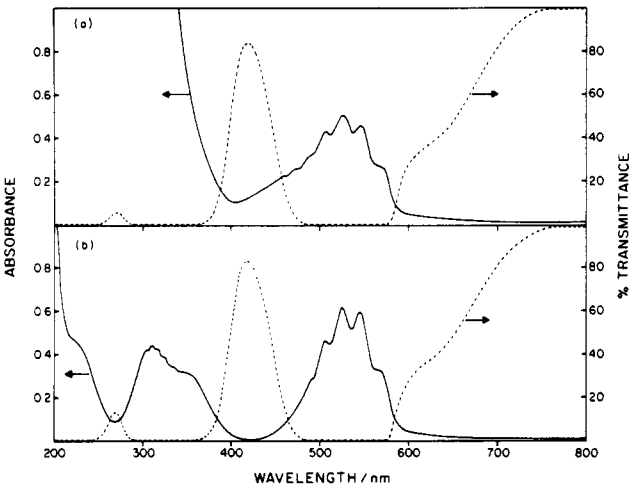

Figure 2. (a) Absorbance spectrum for thermodynamic branch (solid line) and % transmittance spectrum for flow branch (dashed line) at $k_0 = 0.602$ min^{-1}. Path length 1.0 cm. Reactant concentrations and temperature same as Figure 1. (b) Absorbance spectrum of potassium permanganate with $[KMnO_4]_0 = 2.55 \times 10^{-4}$ M (solid line) and % transmittance spectrum with $[KMnO_4]_0 = 2.55 \times 10^{-3}$ M (dashed line). Path length 1.0 cm. Temperature: 25.0 ± 0.1 °C.

report on the discovery and our initial investigation of kinetic bistability in the permanganate oxidation of oxalate. This system was deliberately chosen for study because in batch the rate increases autocatalytically until permanganate is consumed; the reaction then proceeds without autocatalysis. The other known bistable systems also contain autocatalytic and nonautocatalytic reaction pathways.

When oxalate is in stoichiometric excess to permanganate, the reaction proceeds homogeneously to generate manganese(II) and carbon dioxide. The main features of the reaction are accounted for by two processes:

$$MnO_4^- + 4Mn^{2+} + 5nC_2O_4^{2-} + 8H^+ = 5Mn(C_2O_4)_n^{3-2n} + 4H_2O \quad (A)$$

$$2Mn(C_2O_4)_n^{3-2n} = 2Mn^{2+} + (2n-1)C_2O_4^{2-} + 2CO_2 \quad (B)$$

$$n = 1, 2, \text{ or } 3$$

In a definitive study, Noyes and co-workers[4] showed that permanganate and oxalate do not react directly at an appreciable rate, but rather permanganate reacts with an oxalato complex of manganese(II). Permanganate is reduced and Mn(II) is oxidized in a sequence of reactions to generate $Mn(C_2O_4)_n^{3-2n}$, where the value of n depends on the concentration of oxalate. Decomposition of the Mn(III) oxalato complexes in process B is rate determining for the overall reaction, with the monooxalato complex reacting more rapidly than the di or trioxalato complexes.[5] The overall reaction [2A + 5B] is autocatalytic in Mn(II). In a reaction mixture containing only permanganate and oxalate, autocatalysis might be initiated by Mn(II) contaminant in the $KMnO_4$ reagent.

Figure 1 shows the spectrophotometric absorbance at 400 nm as a function of reciprocal residence time (k_0 = flow rate/tank volume) of a reaction mixture within a CSTR pumped with $KMnO_4$ and $Na_2C_2O_4/H_2SO_4$ solutions. Following the conventions of DeKepper, Epstein, and Kustin,[3] we use the terms "thermodynamic branch" and "flow branch" to describe the permanganate–oxalate bistability. At zero flow the system is a batch reaction and the steady state is the state of thermodynamic equilibrium. As the flow rate is increased, the steady state moves continuously along the thermodynamic branch, characterized by a low optical absorbance at 400 nm. The thermodynamic branch remains stable as the flow rate is increased until $k_0 = 0.744$ min^{-1}, where the system undergoes a discontinuous transition to the flow branch. The flow branch is characterized by a higher optical absorbance at 400 nm. In the limit of very high flow rates the reaction mixture composition approaches that of the unreacted reactants. As the flow rate is decreased, the flow branch remains stable until $k_0 = 0.197$ min^{-1}, where the system undergoes a discontinuous transition to the thermodynamic branch. The bistable region is defined by the overlap of the two branches.

Relatively little chemical reaction occurs in the flow branch compared to the thermodynamic branch at a particular flow rate. The UV–VIS spectra for the steady states at $k_0 = 0.602$ min^{-1} are shown in Figure 2a. The spectra of $KMnO_4$ solutions within the CSTR (pumped with distilled water and $KMnO_4$ reagent equal to and $^1/_{10}$ the concentration of that used in the experiment) are shown in Figure 2b. Comparison of the spectra in Figure 2 (dashed lines) shows that in the flow branch $[KMnO_4]$ is about the same as it would be in the absence of any chemical reaction. The spectrum for the thermodynamic branch in Figure 2a (solid line) was analyzed at 350, 420, 450, 525, and 560 nm by using molar absorptivities for MnO_4^- from Figure 2b (solid line) and for $Mn(C_2O_4)_2^-$ and $Mn(C_2O_4)_3^{3-}$ from Adler and Noyes.[4b] The calculated molar absorbance at these wavelengths agrees with the thermodynamic branch spectrum within 3% for $[MnO_4^-] = 1.87 \times 10^{-4}$ M and $[Mn(C_2O_4)_2^-] = 1.17 \times 10^{-3}$ M. The concentration of $Mn(C_2O_4)_3^{3-}$ is not significant for these reaction conditions. Therefore, in the thermodynamic branch at this particular flow rate only 7.3% of the MnO_4^- remains unreacted and about 46% of the manganese is present as $Mn(C_2O_4)_2^-$. The major fraction of the remaining 47% of the manganese is probably $Mn(C_2O_4)$ and $Mn(C_2O_4)^+$. These species do not absorb significantly at the wavelengths used in the above analysis.[4]

Perturbation experiments demonstrated that the flow branch in the bistable region is locally stable. In a typical experiment ($k_0 = 0.394$ min^{-1}), the flow was stopped for 2.5 min, and during this period the absorbance increased from 0.361 to 0.476. When the flow was restored, the absorbance decreased to the original value in about 15 min. Overshoots were observed during supercritical perturbations and during transitions from one branch to another at the hysteresis limits.

A detailed characterization of the permanganate–oxalate bistability will appear with a discussion of the chemical reaction mechanism in a future paper.

Acknowledgment. This work was supported by the National Science Foundation (Grant ISP-8011453-10) and the Research Corporation (Grant 8912).

(3) De Kepper, P.; Epstein, I. R.; Kustin, K. *J. Am. Chem. Soc.*, in press.

(4) (a) Malcolm, J. M.; Noyes, R. M. *J. Am. Chem. Soc.* **1952**, *74*, 2769–2775. (b) Adler, S. J.; Noyes, R. M. *Ibid.* **1955**, *77*, 2036–2042.

(5) Taube, H. *J. Am. Chem. Soc.* **1948**, *70*, 1216–1220.